Chromosome Res (2013) 21:361–374
DOI 10.1007/s10577-013-9362-z

Molecular cytogenetic map of the central bearded dragon, *Pogona vitticeps* (Squamata: Agamidae)

M. J. Young · D. O'Meally · S. D. Sarre · A. Georges · T. Ezaz

Received: 16 February 2013 / Revised: 12 April 2013 / Accepted: 27 April 2013 / Published online: 24 May 2013

Abstract Reptiles, as the sister group to birds and mammals, are particularly valuable for comparative genomic studies among amniotes. The Australian central bearded dragon (*Pogona vitticeps*) is being developed as a reptilian model for such comparisons, with whole-genome sequencing near completion. The karyotype consists of 6 pairs of macrochromosomes and 10 pairs microchromosomes ($2n$=32), including a female heterogametic ZW sex microchromosome pair. Here, we present a molecular cytogenetic map for *P. vitticeps* comprising 87 anchor bacterial artificial chromosome clones that together span each macro- and microchromosome. It is the first comprehensive cytogenetic map for any non-avian reptile. We identified an active nucleolus organizer region (NOR) on the sub-telomeric region of 2q by mapping 18S rDNA and Ag-NOR staining. We identified interstitial telomeric sequences in two microchromosome pairs and the W chromosome, indicating that microchromosome fusion has been a mechanism of karyotypic evolution in Australian agamids within the last 21 to 19 million years. Orthology searches against the chicken genome revealed an intrachromosomal rearrangement of *P. vitticeps* 1q, identified regions orthologous to chicken Z on *P. vitticeps* 2q, snake Z on *P. vitticeps* 6q and the autosomal microchromosome pair in *P. vitticeps* orthologous to turtle *Pelodiscus sinensis* ZW and lizard *Anolis carolinensis* XY. This cytogenetic map will be a valuable reference tool for future gene mapping studies and will provide the framework for the work currently underway to physically anchor genome sequences to chromosomes for this model Australian squamate.

Keywords Reptile · Karyotype · Microchromosome · FISH · Sex chromosome

Abbreviations

APTX	Aprataxin
ATP5A1	ATP synthase, H^+ transporting, mitochondrial F1 complex, alpha subunit 1, cardiac muscle
BAC	Bacterial artificial chromosome
BCL6	B cell CLL/lymphoma 6
BLAST	Basic Local Alignment Search Tool
BLAT	BLAST-like alignment tool
CA10	Carbonic anhydrase X
CHD1	Chromodomain helicase DNA-binding protein 1
CTBP2	C-terminal binding protein 2
CTNNB1	Catenin (cadherin-associated protein), beta 1, 88 kDa
DAPI	4′,6-Diamidino-2-phenylindole

Responsible Editor: Walther Traut.

Electronic supplementary material The online version of this article (doi:10.1007/s10577-013-9362-z) contains supplementary material, which is available to authorized users.

M. J. Young · D. O'Meally · S. D. Sarre · A. Georges · T. Ezaz (✉)
Institute for Applied Ecology, University of Canberra, Canberra, ACT 2601, Australia
e-mail: Tariq.Ezaz@canberra.edu.au

DDX58	DEAD (Asp-Glu-Ala-Asp) box polypeptide 58
DMRT1	Doublesex and mab-3-related transcription factor 1
dUTP	2′-Deoxyuridine 5′-triphosphate
EIF3H	Eukaryotic translation initiation factor 3, subunit H
FAM83B	Family with sequence similarity 83, member B
FBRSL1	Fibrosin-like 1
FISH	Fluorescence in situ hybridization
GHR	Growth hormone receptor
GMPPA	GDP-mannose pyrophosphorylase A
HCRTR2	Hypocretin (orexin) receptor 2
HMGCLL1	3-Hydroxymethyl-3-methylglutaryl-CoA lyase-like 1
IBSP	Integrin-binding sialoprotein
IPO7	Importin 7
IQSEC3	IQ motif and Sec7 domain 3
KAT2B	K(lysine) acetyltransferase 2B
KAT7	K(lysine) acetyltransferase 7
KLF6	Kruppel-like factor 6
NAV2	Neuron navigator 2
NOR	Nucleolus organizer region
NPRL3	Nitrogen permease regulator-like 3
PSMA2	Proteasome (prosome, macropain) subunit, alpha type, 2
RAB5A	RAB5A, member RAS oncogene family
rDNA	Ribosomal DNA
RRM1	Ribonucleotide reductase M1
SRY	Sex-determining region Y
TAX1BP1	Tax1 (human T-cell leukemia virus type I) binding protein 1
TMEM41B	Transmembrane protein 41B
TNFRSF11B	Tumor necrosis factor receptor superfamily, member 11b
TTN	Titin
WAC	WW domain-containing adaptor with coiled coil
ZNF143	Zinc finger protein 143

Introduction

Amniotes are represented by two major lineages: Sauropsida (reptiles and birds) and Synapsida (mammals). The sauropsids are an ancient and incredibly diverse group containing ~18,000 extant species; they are the most species-rich group of amniotes. Within the Sauropsida, squamates (amphisbaenians, lizards and snakes) and the tuatara (Lepidosauria) diverged from turtles, crocodiles and birds (Archosauria) ~275 Mya (Shedlock and Edwards 2009; Fig. 1). The common ancestor of all amniotes existed ~325 Mya in the Carboniferous (Shedlock and Edwards 2009). The availability of amniote genome assemblies, including 60 mammals, and more recently five birds and five reptiles (http://www.ncbi.nlm.nih.gov/genome/browse/), allows comparisons of the organisation and function of amniote genomes across vast evolutionary distances. Whole-genome comparisons have now been made across the three major amniote groups, including among mammals (Chinwalla et al. 2002; Mikkelsen et al. 2007; Warren et al. 2008), between birds and mammals (Hillier et al. 2004), among birds (Dalloul et al. 2010; Warren et al. 2010) and, most recently, between reptiles and birds (Alföldi et al. 2011). These comparisons have given new perspectives on the complex and diverse structure, function and evolution of amniote genomes. However, there are many taxonomic groups, especially squamates, that to date are underrepresented in comparative molecular cytogenetic studies.

Comparative chromosome mapping of genes is a powerful tool for tracing chromosome rearrangements and reconstructing protokaryotypes between distantly related taxa. Reconstruction studies have determined that sauropsid genomes are evolutionarily conserved compared to those of mammals, exhibiting a slow rate of chromosomal rearrangement. This is exemplified by the conserved linkage homology between ancestral amniote and tetrapod protokaryotypes and the chicken karyotype (Kohn et al. 2006; Nakatani et al. 2007; Uno et al. 2012). Within sauropsids, there is strong evolutionary conservation of the macrochromosomes of birds and the Chinese soft-shelled turtle (*Pelodiscus sinensis*; Matsuda et al. 2005; Uno et al. 2012), and among squamates such as the Japanese four-striped rat snake (*Elaphe quadrivirgata*) and the Asian agamid lizard (*Leiolepis reevesii rubritaeniata*; Srikulnath et al. 2009). There is also strong conservation of the avian Z in the karyotypes of turtles, crocodiles and squamates (Kawai et al. 2007; Pokorná et al. 2011).

Reptiles have become a group of great genomic interest in recent years, principally because of their unique phylogenetic position. At present, detailed investigations of chromosomal synteny and comparisons of the genomic characteristics between reptiles

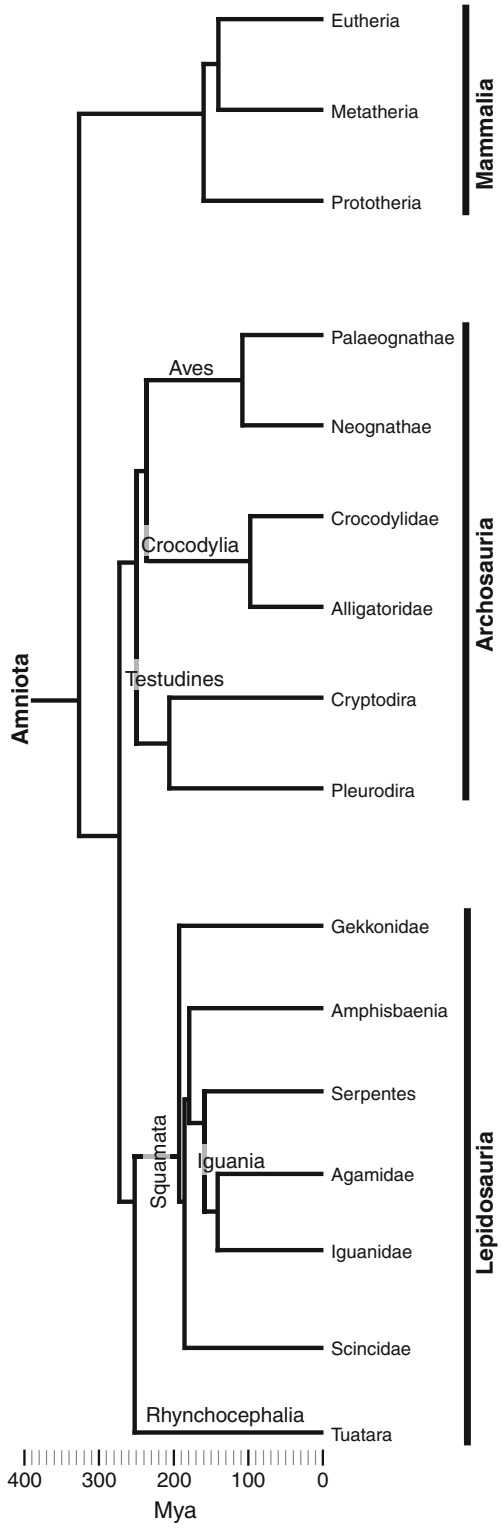

Fig. 1 Amniote phylogeny. Branch lengths are proportional to the divergence dates provided by Hedges et al. (2006) and references therein. Placement of turtles in phylogeny was based on Crawford et al. (2012)

and other amniotes have been restricted to a single species, the North American green anole lizard (*Anolis carolinensis*). Genomic comparisons between *A. carolinensis* and the chicken have revealed considerable differences in genomic characteristics such as genome size, diversity and activity of repetitive elements, GC distribution, and isochore and gene structure (Alföldi et al. 2011; Fujita et al. 2011). However, mapping of genes to *A. carolinensis* chromosomes for the purpose of anchoring genome sequence contigs is not yet complete, and the orthology of most microchromosomes to chicken chromosomes has yet to be demonstrated (Alföldi et al. 2011). In-depth comparative cytogenetic and genomic investigations of the genomes of other non-avian reptiles are required to determine how typical the *A. carolinensis* genome is of squamates and other non-avian reptiles.

There are many important life history traits unique to non-avian reptiles that may in turn shed light on the evolution of life history traits in other amniote taxa. Probably the best studied is reptilian sex determination. Reptiles have evolved a variety of sex-determining mechanisms, and transitions between modes of sex determination have occurred frequently since their divergence with synapsids (Organ and Janes 2008), making them excellent models for understanding the evolution of such mechanisms (Sarre et al. 2004, 2011). Such lability is exemplified in the Australian dragon lizards (Squamata: Agamidae), which exhibit a complex evolutionary history of transitions between genotypic sex determination (GSD) with female heterogamety (ZZ male: ZW female) and temperature-dependent sex determination. Within this group, independent and recent evolution of ZW sex chromosomes has been hypothesized, even between closely related taxa (Ezaz et al. 2009b).

There are approximately 70 species of Australian agamid, all derived from a recent colonisation by an Asian ancestor (~30 Mya; Hugall et al. 2008). One agamid in particular, the Australian central bearded dragon (*Pogona vitticeps*; Ahl 1926), is emerging as a genetic and genomic model, with a whole-genome sequencing project nearing completion. Studies on *P. vitticeps* can give new dimensions to our understanding of complex amniote life history traits and provide much needed comparison to the already sequenced genomes of *A. carolinensis*, turtles, birds and mammals. Within Iguania, *P. vitticeps* and *A. carolinensis* last shared a common ancestor ~144 Mya (Hedges et al. 2006). Evolutionary distances of this scale are useful for

distinguishing between coding and non-coding sequences and identifying regulatory sequences, as has been demonstrated by comparisons of marsupial and eutherian mammal genomes (Wakefield and Graves 2003).

The sex chromosomes of *P. vitticeps* are of particular interest. Sex determination is primarily GSD with female heterogamety and a pair of sex microchromosomes (Ezaz et al. 2005). However, egg incubation at temperature extremes from 34 to 37 °C reverse genotypic males (ZZ) to phenotypic females, demonstrating an interaction between the genotype and temperature in determining sex and that the W chromosome is not necessary for female development (Quinn et al. 2007). Mapping and sequencing of *P. vitticeps* bacterial artificial chromosome (BAC) clones has revealed that *P. vitticeps* ZW sex microchromosomes are non-homologous with snake ZW and bird ZW sex chromosome systems (Ezaz et al. 2009a).

Chromosome characterisation and mapping at the cytogenetic and molecular levels form an essential foundation for genome sequencing projects. Here, we present a detailed characterisation of *P. vitticeps* chromosomes and construct a cytogenetic map with molecular anchor markers spanning all macro- and microchromosomes of the *P. vitticeps* karyotype. We also demonstrate the value of this map for understanding the organisation and evolution of the *P. vitticeps* genome.

Materials and methods

Cell culture and metaphase chromosome preparation

Cell cultures and chromosome preparations were made from short-term whole-blood and primary fibroblast cell cultures as described by Ezaz et al. (2005). Three male and three female *P. vitticeps* were assessed in this study. Cell suspensions were dropped onto slides, air-dried and stored at −80 °C.

Chromosome measurements

The size and arm ratio of each chromosome was determined from ten male and ten female DAPI-stained metaphase spreads. Measurements were taken using the measure-line tool in AxioVision, v4.8.1 (Carl Zeiss Ltd., Cambridge, UK). Chromosome size (in mega base pairs) was calculated relative to the female (A. Amey, personal communication) haploid genome 1.81 pg estimated by MacCulloch et al. (1996), with 1 pg=978 Mbp (Dolezel et al. 2003), giving a total haploid size of 1.77 Mbp.

Probe preparation

In total, we mapped 87 BAC clones to *P. vitticeps* metaphase chromosomes. Sixty-four of these clones were selected randomly from a female *P. vitticeps* 6.2X genomic BAC library (Ezaz et al. 2009a). We also confirmed the locations of 22 *P. vitticeps* clones previously mapped and sequenced by Ezaz et al. (2009b), Patel et al. 2010 and Ezaz et al. (in preparation). A tammar wallaby (*Macropus eugenii*) BAC clone (AGI 329J14) that contains the 18S rDNA locus (O'Meally et al. 2009) was used to map the nucleolus organizer region (NOR). BAC DNA was extracted using the Promega Wizard Plus SV Minipreps DNA Purification System following the manufacturer's protocol, with volumes scaled up for 15-ml cultures.

Fluorescence in situ hybridization

Fluorescence in situ hybridization (FISH) was performed following the protocol described by O'Meally et al. (2009). Approximately 200–500 ng of BAC DNA was directly labelled by nick translation incorporating either Spectrum Orange-dUTP or Spectrum Green-dUTP (Abbott Molecular, Inc., Des Plaines, IL). Three-colour FISH was used, with the third colour generated by the admixture of two labelling reactions (Spectrum Orange-dUTP and Green-dUTP), to produce a yellow hybridization signal. In each case, probes were co-precipitated and resuspended in hybridization buffer. Metaphases were counterstained with DAPI for microscope analysis.

Images of metaphases were captured from 10–20 cells for each hybridization using a Zeiss Axio Scope A1 epifluorescence microscope fitted with a high-resolution microscopy camera AxioCam MRm Rev. 3 (Carl Zeiss Ltd.) and the Vernier coordinates recorded. Images were analysed using AxioVision v4.8.1 software. Multiple rounds of probe hybridization on the same slide were used to clarify ambiguous chromosomal assignments. Coverslips and VectaShield (Vector Laboratories, Burlingame, CA) were removed by washing for 5 min in 2× SSC at room temperature followed by the dehydration of

slides through an ethanol series (70, 90 and 100 % ethanol) and left to air dry. Slides were then aged overnight at −80 °C before probes were re-hybridized. Multiple hybridization images of the same metaphase were merged using Adobe Photoshop, v9.0 (Adobe Systems, Inc.).

Telomere peptide nucleic acid probe

Telomeric repeats were mapped using a Cy3-$(CCCTAA)_3$ peptide nucleic acid (PNA) probe (Bio-Synthesis Inc., Lewisville, TX) as described previously (O'Meally et al. 2009). A BAC clone (237P23) that identifies the Z and W microchromosomes, and which also distinguishes between them through differential hybridisation, was mapped to the same slides after hybridization and washing of the PNA probe as described above.

Silver staining (Ag-NOR)

Ag-NOR staining was performed following the protocol of Howell and Black (1980). Two drops of gelatin solution (2 % gelatin, 1 % formic acid) and four drops of a silver nitrate solution (50 % $AgNO_3$) were added to a slide under a coverslip. The slide was then incubated at 70 °C on a block heater for 2 min until the appearance of a golden brown colour. The slide was then washed in distilled water, counterstained with DAPI and mounted with VectaShield. Images of the metaphases were captured using both fluorescence and bright field microscopy and merged using AxioVision v4.8.1 software.

BAC end sequencing and identification of *P. vitticeps* orthologs

The 64 randomly selected and mapped BAC clones were sequenced using three vector-specific primers: pCC1/pEpiFOS-5 forward sequencing primer (5′-GGATGTGCTGCAAGGCGATTAAGTTGG-3′) and T7 promoter (5′-TAATACGACTCACTATAGGG-3′) and pCC1/pEpiFOS-5 reverse sequencing primer (5′-CTCGTATGTTGTGTGGAATTGTGAGC-3′) (Macrogen Inc., Seoul, South Korea).

BAC end sequences were annotated using BLAT against the *A. carolinensis* whole-genome assembly database (anoCar2: May 2010; http://genome.ucsc.edu). We only considered true hits to be those where one BAC end sequence had more than 100 bp of sequence identity >80 % or where hits from either end of a single BAC lie within 160 Kbp in the *A. carolinensis* assembly. To search more broadly for *P. vitticeps* orthologs, we also used discontiguous megablast (http://blast.ncbi.nlm.nih.gov/) to search the nr database. Hits to genes that were more than 100 bp in length and had an *E* value $\leq 10^{-20}$ were recorded as *P. vitticeps* orthologs. Sequences were not annotated when there were multiple significant but conflicting hits.

The location of chicken orthologs for each *P. vitticeps* gene was determined using Ensembl (http://www.ensembl.org/). For *GMPPA*, *DDX58* and *KAT7*, we used the location of zebra finch orthologs because they were not annotated in the chicken assembly, whilst no orthology of *C19orf47* was identified as it is not annotated in either assembly. One BAC (176G9) was fully sequenced at the Biomolecular Resource Facility (Australian National University, Canberra) using a 3-Kbp mate pair library on 454 (Roche Diagnostics Pty. Ltd., Castle Hill, NSW, Australia) and assembled using the default parameters of Newbler (Roche Diagnostics Pty Ltd.). We determined the genic content of this BAC using Genscan (http://exon.mit.edu/GENSCAN.html) and discontiguous megablast.

Results

The diploid karyotype of *P. vitticeps* contains 32 bi-armed chromosomes — 6 pairs of macrochromosomes and 10 pairs of microchromosomes ($2n$=12M+20m; Witten 1983), including one pair of sex microchromosomes (ZZ male: ZW female; Ezaz et al. 2005). The macrochromosomes consist of five metacentric pairs (first, third, fourth, fifth and sixth) and one submetacentric pair (second); the microchromosomes are all metacentric (Fig. 2).

Chromosomes 1, 2, 5 and 6 were distinguished morphologically by size and centromere position. Chromosomes 3 and 4 were relatively similar in morphology, and owing to an infrequent polymorphism in the size of chromosome 3, unequivocal pairing of homologs was not always possible. The largest microchromosome (pair 7) was distinguished from other microchromosomes by size. Other microchromosome pairs (8–14 and ZW) were difficult to distinguish by size and centromere position. Distinguishing between the *p* and *q* arms of chromosomes 3 and 4 and each of the microchromosomes was not always possible because the centromeric index was so close to 0.5 (Table 1).

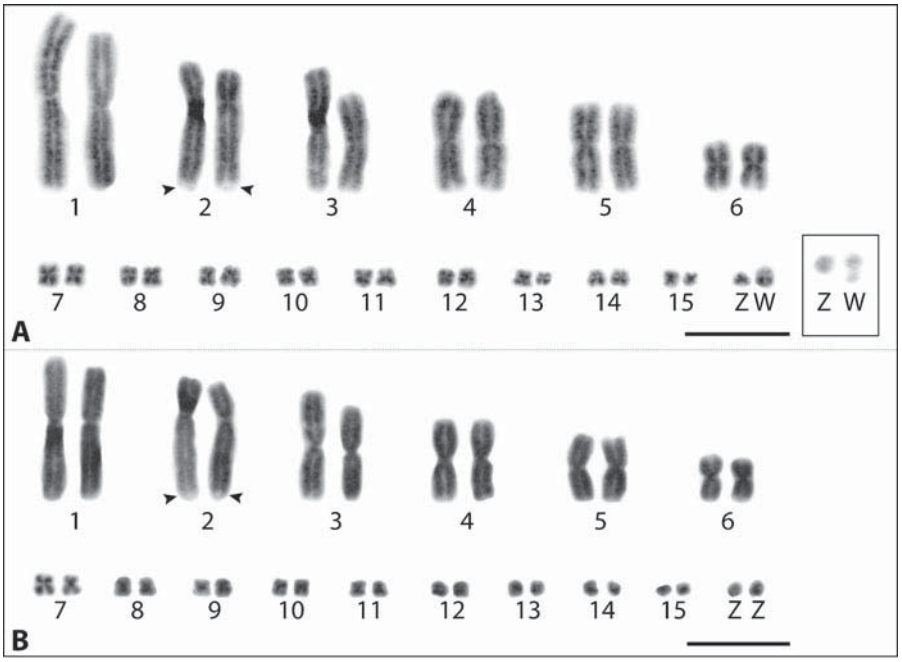

Fig. 2 DAPI-stained karyotypes from a female (**a**) and male (**b**) *P. vitticeps*. The karyotype consists of 6 pairs of macrochromosomes (*1–6*) and 10 pairs of microchromosomes (*7–15*) and a pair of ZW sex microchromosomes (2*n*=32). The sex chromosomes are heteromorphic, with the W chromosome substantially larger than the Z. In some metaphases, W is uncoiled and clearly heteromorphic (*inset* in **a**). Chromosome 3 shows an autosomal polymorphism in one homolog. *Arrowheads* indicate the secondary constriction at the site of the NOR on chromosome 2q. Sex chromosomes were identified by FISH mapping of a diagnostic BAC clone (237P23). *Scale bars*, 10 μm

A single NOR was identified at the secondary constriction in the sub-telomeric region of 2q by FISH mapping of a BAC clone containing the 18S rDNA gene and Ag-NOR staining. Signals on both homologs consistently mapped to the same location with similar intensity (Fig. 3a, b).

Mapping of the PNA telomeric probe Cy3-$(CCCTAA)_3$ identified telomeres at the ends of each chromosome and interstitial telomeric sequences within microchromosome pairs 7 and 8 and the W chromosome. Hybridization signals were not always of equal intensity on homologous chromosome arms (Fig. 4).

Eighty-seven BAC clones were mapped to chromosomes of *P. vitticeps* using multicolour FISH (Fig. 5). Sixty-four of the 87 BAC clones mapped to macrochromosomes and 23 to microchromosomes. We identified anchor BAC clones that are diagnostic for each arm of all macrochromosomes and putatively for each separate microchromosome (Fig. 6 and Table 2 and Electronic supplementary materials Table 1). Anchor BACs were assigned to microchromosomes based on chromosome size measurements and reciprocal multicolour FISH mapping. Each of the diagnostic BAC clones mark a single chromosome pair, except those that map to the Z and W microchromosomes, which also show a diffuse signal pattern on the sub-telomeric region of 2q (Fig. 3c).

We estimated the total female *P. vitticeps* genome size to be 1.77 Gbp. We collected 44.8 Kbp of the BAC sequence from 64 clones (NCBI Genbank accession nos. JY473859–JY474041) and annotated 22 genes (Table 2). The average GC content of BAC sequences that map to macrochromosomes (42.07 %, SD=5.13) is not significantly lower than those that map to microchromosomes (43.62 %, SD=5.57; *t* test: $p=0.20$).

Discussion

Cytogenetic map of *P. vitticeps* and chromosome homology

Detailed cytogenetic maps based on standardized chromosome ideograms, with molecular anchor markers on each chromosome, are valuable tools for investigating the organisation and evolution of

Table 1 Chromosome dimensions of the *P. vitticeps* karyotype

Chromosome	*p*	SE	Range	*q*	SE	Range	CI	% Haploid length	Chromosome size (Mbp)
Macrochromosomes									
1	8.40	0.12	4.36–8.25	9.58	0.11	4.65–8.68	0.47	17.98	318.21
2	4.92	0.07	2.69–5.00	11.45	0.12	6.10–12.00	0.30	16.36	289.63
3	6.59	0.08	3.55–7.64	6.87	0.10	3.59–8.42	0.49	13.46	238.22
4	5.87	0.05	3.20–6.00	6.12	0.05	3.15–6.18	0.49	11.99	212.29
5	4.72	0.05	2.58–4.03	5.34	0.06	2.83–4.79	0.47	10.07	178.21
6	3.04	0.03	1.83–2.63	3.68	0.04	2.02–4.07	0.45	6.72	118.92
Microchromosomes									
7	1.37	0.02	0.79–1.07	1.65	0.03	0.91–1.33	0.45	3.02	53.49
8	1.27	0.02	0.69–1.02	1.44	0.02	0.78–1.24	0.47	2.71	48.00
9	1.22	0.02	0.72–1.01	1.35	0.02	0.78–1.14	0.47	2.57	45.50
10	1.18	0.02	0.65–0.93	1.28	0.02	0.72–1.02	0.48	2.46	43.61
11	1.12	0.02	0.66–0.87	1.23	0.02	0.71–1.04	0.48	2.35	41.65
12	1.08	0.02	0.65–0.85	1.18	0.02	0.69–1.04	0.48	2.26	39.99
13	1.03	0.02	0.58–0.84	1.14	0.02	0.65–1.03	0.47	2.17	38.33
14	0.96	0.02	0.49–0.84	1.05	0.02	0.52–0.88	0.48	2.01	35.52
15	0.83	0.02	0.32–0.74	0.95	0.02	0.49–0.87	0.47	1.78	31.49
Sex chromosomes									
Z	0.86	0.03	0.41–0.69	1.08	0.03	0.53–1.02	0.44	1.94	34.28
W	1.18	0.04	0.73–0.84	1.40	0.05	0.87–1.16	0.46	2.58	45.64

The length of each chromosome arm was measured and averaged for ten male and ten female DAPI-stained metaphase spreads. The centromeric index (CI) is the ratio of the *p* arm to the length of the chromosome. Measurements were taken from metaphases that had the sex microchromosomes identified by FISH mapping of a diagnostic BAC that marks the Z and W chromosomes differentially (237P23) so that, in all, 30 Zs and 10 Ws were measured

genomes. Physically anchoring loci in bird and reptilian genomes has proven to be particularly difficult as the microchromosome complement can be difficult to distinguish, both morphologically and cytologically. We present the first complete BAC-anchored cytogenetic map with 87 markers assigned to each macrochromosome

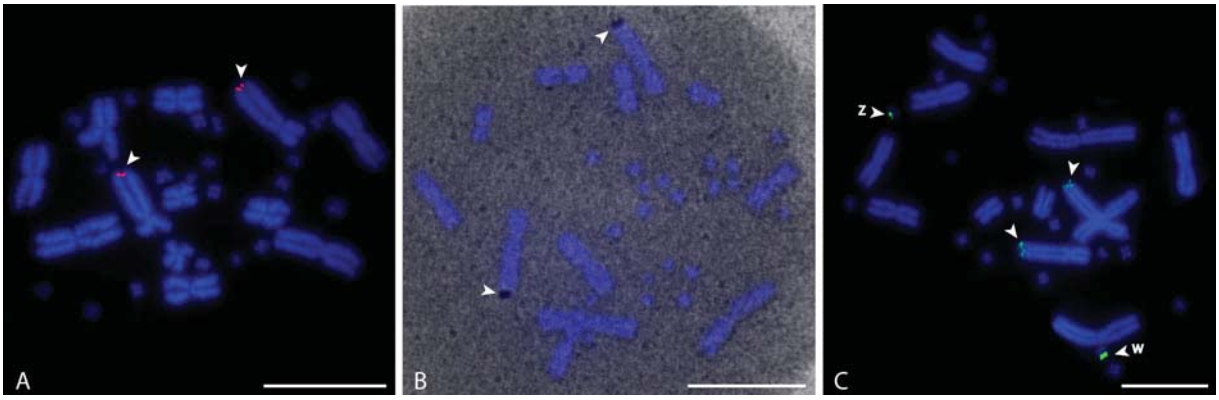

Fig. 3 **a** 18S rDNA mapping by FISH of *M. eugenii* BAC clone 329J14 (*red*) on *P. vitticeps* metaphase chromosomes. *Arrowheads* indicate the position of the NOR on 2q. **b** Ag-NOR staining identifying the presence of an active NOR on 2q (*arrowheads*). **c** BAC clone 237P23 (*green*) marking the Z and W sex microchromosome pair as well as the subtelomeric region of chromosome 2q. Metaphase chromosomes are counterstained with DAPI. *Scale bars*, 10 μm

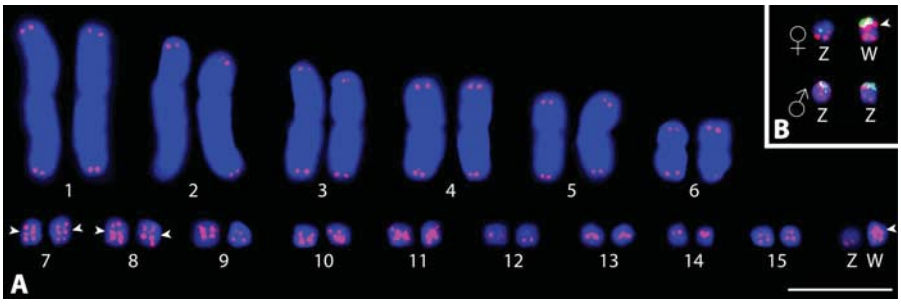

Fig. 4 **a** Karyotype of chromosomes from a female *P. vitticeps*. The telomeric probe (*red*) reveals telomeres at the ends of all chromosomes as well as interstitial telomeric sequences in microchromosome pairs 7 and 8 and on an unpaired microchromosome homolog (*arrowheads*), indicating that they have likely arisen recently by fusion events. **b** Hybridization of the telomeric probe (*red*) with a diagnostic BAC (237P23, *green*) identifies the W sex chromosome as the unpaired homolog with interstitial telomeric sequences. *Scale bar*, 10 μm

arm and each microchromosome for a non-avian reptile (Fig. 6). These BAC clones represent a valuable resource for the work currently underway to physically anchor *P. vitticeps* whole-genome sequence scaffolds to chromosomes. Even with this low-resolution map, our physical markers have identified the orthology of most *P. vitticeps* chromosomes to those of the chicken (Fig. 6) and regions of conserved synteny and rearrangements between *P. vitticeps* and other reptiles.

Chromosome painting has demonstrated that *P. vitticeps* chromosome 1 is orthologous to chicken chromosomes 3, 5 and 7 (Pokorná et al. 2012). Our physical mapping of BACs bearing orthologs of *HMGCLL1*, *HCRTR2* and *FAM83B* to *P. vitticeps* 1p and *TTN*, *ZNF143*, *IPO7*, *TMEM41B* and *GMPPA* to *P. vitticeps* 1q confirms this. From a wider taxonomic perspective, the synteny of this large bi-armed chromosome representing chicken chromosomes 3, 5 and 7 is also conserved across most major squamate lineages (Pokorná et al. 2012). Our mapping data have revealed an internal rearrangement in *P. vitticeps* 1q. This rearrangement was likely a paracentric inversion or translocation, whereby the insertion of regions on *P. vitticeps* 1q orthologous to chicken chromosome 5 caused a break in gene order between the regions orthologous to chicken chromosome 7. Similarly, *A. carolinensis* chromosome 1 shares orthology with chicken chromosomes 3, 5 and 7 and shows the same

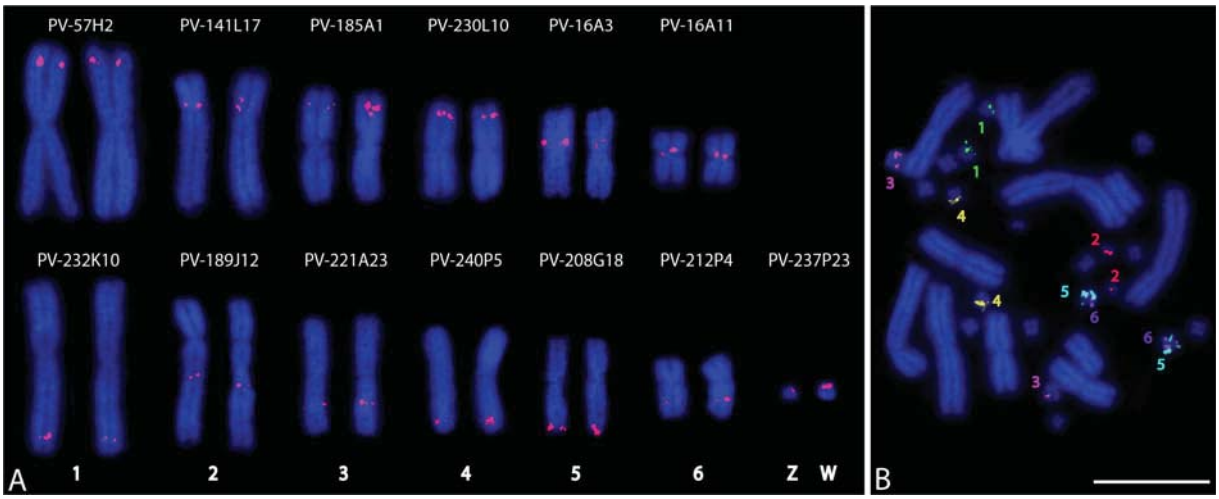

Fig. 5 **a** Anchor BAC mapping by FISH to single locations across *P. vitticeps* macrochromosomes and the ZW microchromosome pair. Clone ID is given *above each chromosome pair*. **b** Reciprocal multicolour FISH mapping of six microchromosome BAC clones onto the same metaphase. *1*, 221B16 (*green*); *2*, 16A10 (*red*); *3*, 197P21 (*magenta*); *4*, 230K11 (*yellow*); *5*, 232P19 (*aqua*); *6*, 105P18 (*purple*). *Scale bar*, 10 μm

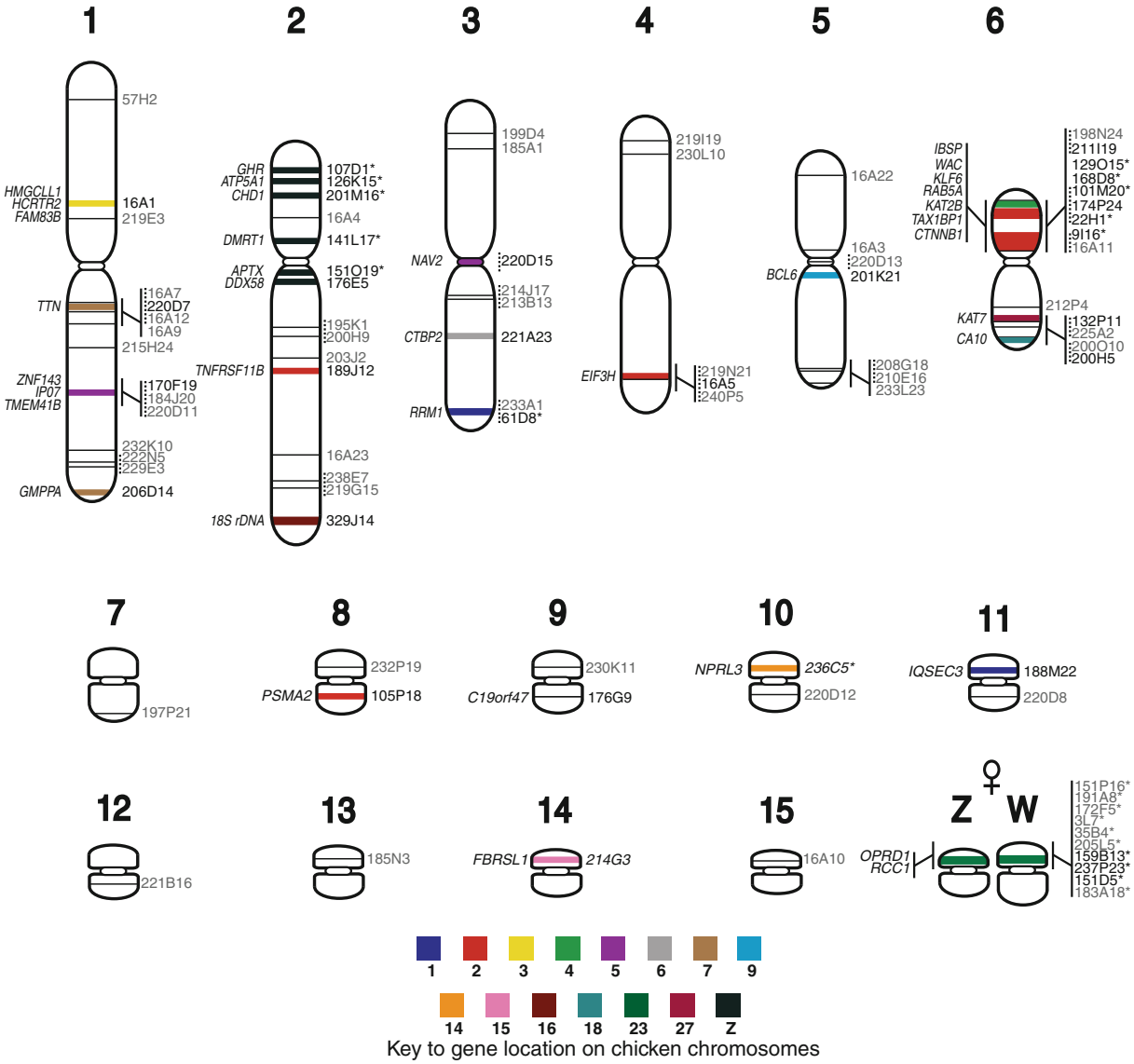

Fig. 6 *P. vitticeps*–chicken comparative map. BAC clones were mapped by FISH to *Pogona* chromosomes. Clone numbers are shown to the *right of chromosomes* at their mapped locations; gene symbols to the *left*. Gene symbols are those listed by the HUGO Gene Nomenclature Committee (http://www.genenames.org/). *Colour key* indicates homology to chicken chromosomes. Clone numbers and gene symbols joined by a *dotted line* indicate that the order of these clones and the genes they contain is unknown on the chromosome. *Asterisk* denotes clones mapped in a previous study

break in gene order in the region orthologous to chicken chromosome 7 (Alföldi et al. 2011), suggesting that this rearrangement is at least 144 Mya. The distal location of *GMPAA* in *P. vitticeps* and the medial location of chicken chromosome 7 orthologs in *A. carolinensis* suggest that subsequent lineage-specific rearrangements have occurred.

Physical mapping of BACs and chromosome painting have identified regions of *P. vitticeps* chromosome 2 that are orthologous to chicken Z (Ezaz et al. 2009a; Pokorná et al. 2011). However, whether the entire chromosome or only the short arm is orthologous to the avian Z has remained unclear. Our physical mapping of *DDX58* in conjunction with another BAC

Table 2 Gene content and chromosome locations of BAC clones in *P. vitticeps*

Library ID	Reference	Clone ID	Gene symbol	Chromosomal location
PV, *Pogona vitticeps* (central bearded dragon)	This study	16A1	*HMGCLL1*; *FAM83B*; *HCRTR1*	1p
		220D7	*TTN*	1q
		170F19	*ZNF143*; *IPO7*; *TMEM41B*	1q
		206D14	*GMPPA*	1q
		176E5	*DDX58*	2q
		189 J12	*TNFRSF11B*	2q
		185A1	_	3p
		220D15	*NAV2*	3*
		221A23	*CTBP2*	3q
		230L10	–	4p
		16A5	*EIF3H*	4q
		16A22	–	5p
		201K21	*BCL6*	5q
		211I19	*IBSP*	6p
		174P24	*KAT2B*	6p
		132P11	*MYST2*	6q
		200H5	*CA10*	6q
		197P21	–	7
		105P18	*PSMA2*	8
		176G9	*C19orf47*	9
		188M22	*IQSEC3*	11
		221B16	–	12
		185N3	–	13
		214G3	*FBRSL1*	14
		16A10	–	15
	Ezaz et al. (2009b)	107D1	*GHR*	2p
		126K15	*ATP5A1*	2p
		201M16	*CHD1*	2p
		141L17	*DMRT1*	2p
		151O19	*APTX*	2q
		129O15	*WAC*	6p
		168D8	*KLF6*	6p
		101M20	*RAB5A*	6p
		22H1	*TAX1BP1*	6p
		9I16	*CTNNB1*	6p
	Patel et al. (2010)	61D8	*RRM1*	3q
		236C5	*NPRL3*	10
	Ezaz et al., in preparation	159B13	*OPRD1*, *RCC1*	Zp; Wp
		237P23	*OPRD1*, *RCC1*	Zp; Wp
		151D5	*OPRD1*, *RCC1*	Zp; Wp
AGI, *Macropus eugenii* (tammar wallaby)	O'Meally et al. (2009)	329J14	*18S rDNA*	2q

A total of 37 genes have been mapped to the chromosomes of *Pogona*, in this study or by Ezaz et al. (2009b), Patel et al. (2010) or Ezaz et al. (in preparation). Where BAC clones have been uniquely mapped to a chromosome or chromosome arm but no genes have been identified, we report diagnostic clones only

mapped in a previous study by Ezaz et al. (2009b) bearing *APTX*, suggest that both arms of chromosome 2 have regions of orthology with the avian Z. In any case, our mapping of *DDX58* has extended the region on 2q orthologous with the avian Z (Fig. 6). Orthology of *P. vitticeps* 6p with chicken 2 and snake Z has been demonstrated by BAC mapping (Ezaz et al. 2009a). Our mapping of *KAT7* on *P. vitticeps* 6q has extended the region orthologous to the snake Z from the short arm of chromosome 6 to include a region on the long arm of this chromosome (Fig. 6).

Whilst each *P. vitticeps* microchromosome has a diagnostic anchor BAC marker, limited genic information meant that we could only identify the orthology of the ZW microchromosomes and four autosomal microchromosomes to chicken chromosomes (Fig. 6). Physical mapping of *FBRSL1* suggests that *P. vitticeps* chromosome 14 is orthologous to chicken chromosome 15 and, therefore, orthologous to Chinese soft-shelled turtle *P. sinensis* ZW (Kawagoshi et al. 2009) and *A. carolinensis* XY sex chromosomes (O'Meally et al. 2012). We physically mapped the BAC clone bearing *FBRSL1* and a *P. vitticeps* ZW clone bearing *OPRD1* and *RCC1* using multicolour FISH to separate microchromosomes, confirming the non-homology of these sex chromosome systems (Fig. 6).

Two *P. vitticeps* microchromosomes (8 and 11) share an ortholog each with chicken macrochromosomes 2 and 1, respectively (Fig. 6). This contrasts with the reconstruction of ancestral tetrapod and amniote protokaryotypes which show that chicken microchromosomes represent ancient syntenic blocks, which are generally conserved in squamates (Uno et al. 2012). These blocks are likely to be conserved in *P. vitticeps*, particularly as chicken microchromosomes 10, 11, 15, 19, 24 and 28 are orthologous to microchromosomes of the agamid *L. r. rubritaeniata* (Srikulnath et al. 2009), which shared an ancestor with *P. vitticeps* ~89 Mya (Hedges et al. 2006). However, even though microchromosome rearrangements in squamate lineages have occurred primarily by the fusion of macro- and microchromosomes (Uno et al. 2012), some *P. vitticeps* and *L. r. rubritaeniata* microchromosomes are orthologous to chicken macrochromosomes (Fig. 6; Srikulnath et al. 2009). Further gene mapping will indicate whether these microchromosomes arose by fission of macrochromosomes or translocations of these genes to existing microchromosomes. The diagnostic BACs we have identified for each microchromosome will, in combination with whole-genome sequence scaffolds, identify conserved synteny of *P. vitticeps* microchromosomes with those of other sauropsids.

Evolution of the *P. vitticeps* karyotype

The *P. vitticeps* karyotype ($2n$=32; 12M+20m), first described by Witten (1983), is typical of most agamids within the Australian radiation (Olmo and Signorino 2005; Witten 1983; Fig. 2). Similar karyotypes, but with two additional microchromosome pairs ($2n$=36; 12M+24m), are relatively conserved in the Australian agamids *Physignathus* and *Hypsilurus* (Olmo and Signorino 2005; Witten 1983) and Asian agamids (Olmo and Signorino 2005). These genera represent basal members of the Australian agamid phylogeny (Hugall et al. 2008) and therefore likely retain the ancestral genome structure. The $2n$=36 karyotype comprising 12 bi-armed macrochromosomes and 24 microchromosomes is common in the suborder Iguania and represents an ancestral organisation (Olmo and Signorino 2005; Paull et al. 1976). Our mapping of 18S rDNA to *P. vitticeps* 2q has also revealed that *P. vitticeps* retains the ancestral position of the NOR for Iguania (Fig. 3a, b), which is located on chromosome 2 or a pair of microchromosomes across this group (Porter et al. 1991).

Through comparisons of chromosome number and macrochromosome morphology between Australian agamids, Witten (1983) hypothesised that evolution of the derived Australian agamid karyotype of $2n$=32 had occurred through microchromosome fusion. Our physical mapping of telomeric sequences in *P. vitticeps* has provided molecular evidence validating this theory of microchromosomal fusion as interstitial telomeric sequences were observed in microchromosome pairs 7 and 8 (Fig. 4). Interstitial telomeric sequences may be indicative of ancestral chromosome rearrangements such as fusions or inversions (Meyne et al. 1990; Ruiz-Herrera et al. 2008). Following fusion of the separate microchromsoomes, one of the centromeres was lost in each pair. Tracing the provenance of the 12M+20m karyotype through the Australian agamid phylogeny (Hugall et al. 2008; Olmo and Signorino 2005; Witten 1983) indicates that both fusion events occurred 21–19 Mya.

The size heteromorphy of *P. vitticeps* chromosome 3 is evident in approximately 50 % of both male and female karyotypes; therefore, duplications, differential

contraction or indels are likely responsible rather than any sex-related chromosome heteromorphism. A total of eight BAC clones were mapped to chromosome 3 and five to chromosome 4, allowing for reliable and unambiguous identification of these chromosomes for assigning physical loci in future mapping studies.

The ZW sex microchromosomes of *P. vitticeps* have been proven difficult to distinguish from other microchromosomes and have therefore been referred to as cryptic and homomorphic (Ezaz et al. 2005). In this study, physical mapping of BAC clones has allowed for reproducible and unambiguous identification of both the Z and W microchromosomes, which, for the first time, has enabled size comparison between them. The W chromosome is 11.8 Mbp larger than the Z (Table 1). In amniotes, the W or Y chromosome is typically smaller than their Z or X counterpart, but *P. vitticeps* joins a collection of species where the reverse is true (e.g. the Australian Murray river turtle, *Emydura macquarii*; Martinez et al. 2008). The elongation of the W chromosome may be due to the accumulation of transposable elements and other repetitive DNA in the absence of recombination, which has yet to be counterbalanced by substantial neutral deletions typical of degenerated W or Y chromosomes. However, our physical mapping of telomeric sequence has identified interstitial telomeric sequences within the W homolog (Fig. 4) and suggests that the difference in size between Z and W has arisen either through fusion of a chromosomal fragment onto the W homolog or through amplification of telomeric sequences at a fragile site break on the W. The diffuse hybridization of ZW BACs on the telomeric region of 2q may provide evidence as to the provenance of the genomic fragment that fused with the W chromosome (Fig. 3).

GC composition

Our estimate of the genome-wide GC content for *P. vitticeps* is 42.3 % (SD=5.21) from BAC end sequences. The GC content of BAC ends that map to macrochromosomes (42.07 %, SD=5.13) did not significantly differ from those that map to microchromosomes (43.62 %, SD=5.58; *t* test: $p=0.20$). However, reverse fluorescent staining suggests that *P. vitticeps* microchromosomes are GC-rich compared with macrochromosomes (Ezaz et al. 2005) and that *P. vitticeps* has chromosome size-dependent GC compartmentalization similar to archosaurs (Hillier et al. 2004; Kasai et al. 2012; Kuraku et al. 2006) and snakes (Matsubara et al. 2012). The BAC-anchored *P. vitticeps* cytogenetic map we have developed will be valuable for discovering trends in GC compartmentalization and many other genomic characteristics once the work currently underway to anchor whole-genome sequences to chromosomes is completed.

Conclusion

We have developed a BAC-anchored cytogenetic map for *P. vitticeps* based on a standardized chromosome ideogram and chromosome characterization at the cytogenetic and molecular levels. Here, we have demonstrated the value of this tool for investigating the organisation and evolution of the *P. vitticeps* genome. We identified an intrachromosomal rearrangement in *P. vitticeps* 1q and two microchromosome fusion events through mapping of BACs and telomeric sequences. We extended the identified regions homologous to the chicken Z on chromosome 2 and the snake Z on chromosome 6. Furthermore, we identified the *P. vitticeps* microchromosome orthologous to Chinese soft-shelled turtle *P. sinensis* ZW and lizard *A. carolinensis* XY sex chromosomes and established that these sex chromosomes are independent of *P. vitticeps* ZW. The anchor BACs represent valuable reference markers for future gene mapping studies. The cytogenetic map will provide a critical framework for the work currently underway to physically anchor genome sequences to chromosomes for the completion of the *P. vitticeps* genome map for this model Australian squamate.

Acknowledgments This work was funded by an ARC DP awarded to SD, AG and Scott Edwards, as was the purchase of the *P. vitticeps* BAC Library. This work was undertaken by MY as a Bachelor of Applied Science Honours with the Institute of Applied Ecology at the University of Canberra. We would like to thank Jacqui Richardson and Alistair Zealey for their care of captive animals and Juliet Ward for laboratory assistance.

References

Ahl E (1926) Neue Eidechsen und Amphibien. Zoologischer Anzeiger 67:186–192

Alföldi J, Di Palma F, Grabherr M, Williams C, Kong L, Mauceli E, Russell P, Lowe CB, Glor RE, Jaffe JD (2011) The genome of the green anole lizard and a comparative analysis with birds and mammals. Nature 477:587–591

Chinwalla AT, Cook LL, Delehaunty KD, Fewell GA, Fulton LA, Fulton RS, Graves TA, Hillier LDW, Mardis ER, McPherson JD (2002) Initial sequencing and comparative analysis of the mouse genome. Nature 420:520–562

Crawford NG, Faircloth BC, McCormack JE, Brumfield RT, Winker K, Glenn TC (2012) More than 1000 ultraconserved elements provide evidence that turtles are the sister group of archosaurs. Biol Lett 8:783–786

Dalloul RA, Long JA, Zimin AV, Aslam L, Beal K, Bouffard P, Burt DW, Crasta O, Crooijmans RPMA, Cooper K (2010) Multi-platform next-generation sequencing of the domestic turkey (*Meleagris gallopavo*): genome assembly and analysis. PLoS Biology 8:e1000475

Dolezel J, Bartos J, Voglmayr H, Greilhuber J (2003) Nuclear DNA content and genome size of trout and human. Cytometry Part A: The Journal of the International Society for Analytical Cytology 51:127

Ezaz T, Moritz B, Waters P, Marshall Graves JA, Georges A, Sarre SD (2009a) The ZW sex microchromosomes of an Australian dragon lizard share no homology with those of other reptiles or birds. Chromosome Res 17:965–973

Ezaz T, Quinn AE, Miura I, Sarre SD, Georges A, Graves JAM (2005) The dragon lizard *Pogona vitticeps* has ZZ/ZW micro-sex chromosomes. Chromosome Res 13:763–776

Ezaz T, Quinn AE, Sarre SD, O'Meally D, Georges A, Marshall Graves JA (2009b) Molecular marker suggests rapid changes of sex-determining mechanisms in Australian dragon lizards. Chromosome Res 17:91–98

Fujita MK, Edwards SV, Ponting CP (2011) The *Anolis* lizard genome: an amniote genome without isochores. Genome Biol Evol 3:974

Hedges SB, Dudley J, Kumar S (2006) TimeTree: a public knowledge-base of divergence times among organisms. Bioinformatics 22:2971–2972

Hillier LDW, Miller W, Birney E, Warren W, Hardison RC, Ponting CP, Bork P, Burt DW, Groenen MAM, Delany ME (2004) Sequence and comparative analysis of the chicken genome provide unique perspectives on vertebrate evolution. Nature 432:695–716

Howell WM, Black DA (1980) Controlled silver-staining of nucleolus organizer regions with a protective colloidal developer: a 1-step method. Experientia 36:1014–1015

Hugall AF, Foster R, Hutchinson M, Lee MSY (2008) Phylogeny of Australasian agamid lizards based on nuclear and mitochondrial genes: implications for morphological evolution and biogeography. Biol J Linn Soc 93:343–358

Kasai F, O'Brien PCM, Ferguson-Smith MA (2012) Reassessment of genome size in turtle and crocodile based on chromosome measurement by flow karyotyping: close similarity to chicken. Biol Lett 8:631–635

Kawagoshi T, Uno Y, Matsubara K, Matsuda Y, Nishida C (2009) The ZW micro-sex chromosomes of the Chinese soft-shelled turtle (*Pelodiscus sinensis*, Trionychidae, Testudines) have the same origin as chicken chromosome 15. Cytogenet Genome Res 125:125–131

Kawai A, Nishida-Umehara C, Ishijima J, Tsuda Y, Ota H, Matsuda Y (2007) Different origins of bird and reptile sex chromosomes inferred from comparative mapping of chicken Z-linked genes. Cytogenet Genome Res 117:92–102

Kohn M, Högel J, Vogel W, Minich P, Kehrer-Sawatzki H, Graves JAM, Hameister H (2006) Reconstruction of a 450-My-old ancestral vertebrate protokaryotype. Trends Genet 22:203–210

Kuraku S, Ishijima J, Nishida-Umehara C, Agata K, Kuratani S, Matsuda Y (2006) cDNA-based gene mapping and GC 3 profiling in the soft-shelled turtle suggest a chromosomal size-dependent GC bias shared by sauropsids. Chromosome Res 14:187–202

MacCulloch RD, Upton DE, Murphy RW (1996) Trends in nuclear DNA content among amphibians and reptiles. Comp Biochem Physiol B Biochem Mol Biol 113:601–605

Martinez PA, Ezaz T, Valenzuela N, Georges A, Marshall Graves JA (2008) An XX/XY heteromorphic sex chromosome system in the Australian chelid turtle *Emydura macquarii*: a new piece in the puzzle of sex chromosome evolution in turtles. Chromosome Res 16:815–825

Matsubara K, Kuraku S, Tarui H, Nishimura O, Nishida C, Agata K, Kumazawa Y, Matsuda Y (2012) Intra-genomic GC heterogeneity in sauropsids: evolutionary insights from cDNA mapping and GC3 profiling in snake. BMC Genomics 13:604

Matsuda Y, Nishida-Umehara C, Tarui H, Kuroiwa A, Yamada K, Isobe T, Ando J, Fujiwara A, Hirao Y, Nishimura O (2005) Highly conserved linkage homology between birds and turtles: bird and turtle chromosomes are precise counterparts of each other. Chromosome Res 13:601–615

Meyne J, Baker RJ, Hobart HH, Hsu T, Ryder OA, Ward OG, Wiley JE, Wurster-Hill DH, Yates TL, Moyzis RK (1990) Distribution of non-telomeric sites of the $(TTAGGG)_n$ telomeric sequence in vertebrate chromosomes. Chromosoma 99:3–10

Mikkelsen TS, Wakefield MJ, Aken B, Amemiya CT, Chang JL, Duke S, Garber M, Gentles AJ, Goodstadt L, Heger A (2007) Genome of the marsupial *Monodelphis domestica* reveals innovation in non-coding sequences. Nature 447:167–177

Nakatani Y, Takeda H, Kohara Y, Morishita S (2007) Reconstruction of the vertebrate ancestral genome reveals dynamic genome reorganization in early vertebrates. Genome Res 17:1254–1265

O'Meally D, Miller H, Patel H, Marshall Graves JA, Ezaz T (2009) The first cytogenetic map of the tuatara, *Sphenodon punctatus*. Cytogenet genome res 127:213–223

O'Meally D, Ezaz T, Georges A, Sarre SD, Graves JA (2012) Are some chromosomes particularly good at sex? Insights from amniotes. Chromosome Res 20:7–19

Olmo E, Signorino G (2005) Chromorep: a reptile chromosomes database. http://chromorep.univpm.it. Accessed 7 May 2013

Organ CL, Janes DE (2008) Evolution of sex chromosomes in Sauropsida. Integr Comp Biol 48:512–519

Patel VS, Ezaz T, Deakin JE, Marshall Graves JA (2010) Globin gene structure in a reptile supports the transpositional model for amniote α- and β-globin gene evolution. Chromosome Res 18:897–907

Paull D, Williams EE, Hall WP (1976) Lizard karyotypes from the Galapagos Islands: chromosomes in phylogeny and evolution. Breviora 441:1–31

Pokorná M, Giovannotti M, Kratochvíl L, Caputo V, Olmo E, Ferguson-Smith MA, Rens W (2012) Conservation of chromosomes syntenic with avian autosomes in squamate reptiles revealed by comparative chromosome painting. Chromosoma 121:409–418

Pokorná M, Giovannotti M, Kratochvíl L, Kasai F, Trifonov VA, O'Brien PCM, Caputo V, Olmo E, Ferguson-Smith MA,

Rens W (2011) Strong conservation of the bird Z chromosome in reptilian genomes is revealed by comparative painting despite 275 million years divergence. Chromosoma 120:455–468

Porter CA, Hamilton MJ, Sites Jr JW, Baker RJ (1991) Location of ribosomal DNA in chromosomes of squamate reptiles: systematic and evolutionary implications. Herpetologica 47:271–280

Quinn AE, Georges A, Sarre SD, Guarino F, Ezaz T, Graves JAM (2007) Temperature sex reversal implies sex gene dosage in a reptile. Science 316:411–411

Ruiz-Herrera A, Nergadze S, Santagostino M, Giulotto E (2008) Telomeric repeats far from the ends: mechanisms of origin and role in evolution. Cytogenet Genome Res 122:219–228

Sarre SD, Ezaz T, Georges A (2011) Transitions between sex-determining systems in reptiles and amphibians. Annu Rev Genom Hum Genet 12:391–406

Sarre SD, Georges A, Quinn A (2004) The ends of a continuum: genetic and temperature-dependent sex determination in reptiles. BioEssays 26:639–645

Shedlock AM, Edwards SV (2009) Amniotes (amniota). In: Hedges SB, Kumar S (eds) The timetree of life. Oxford University Press, New York, pp 375–379

Srikulnath K, Nishida C, Matsubara K, Uno Y, Thongpan A, Suputtitada S, Apisitwanich S, Matsuda Y (2009) Karyotypic evolution in squamate reptiles: comparative gene mapping revealed highly conserved linkage homology between the butterfly lizard (*Leiolepis reevesii rubritaeniata*, Agamidae, Lacertilia) and the Japanese four-striped rat snake (*Elaphe quadrivirgata*, Colubridae, Serpentes). Chromosome Res 17:975–986

Uno Y, Nishida C, Tarui H, Ishishita S, Takagi C, Nishimura O, Ishijima J, Ota H, Kosaka A, Matsubara K (2012) Inference of the protokaryotypes of amniotes and tetrapods and the evolutionary processes of microchromosomes from comparative gene mapping. PLoS One 7:e53027

Wakefield MJ, Graves JAM (2003) The kangaroo genome. EMBO Rep 4:143–147

Warren WC, Clayton DF, Ellegren H, Arnold AP, Hillier LDW, Künstner A, Searle S, White S, Vilella AJ, Fairley S (2010) The genome of a songbird. Nature 464:757–762

Warren WC, Hillier LDW, Graves JAM, Birney E, Ponting CP, Grützner F, Belov K, Miller W, Clarke L, Chinwalla AT (2008) Genome analysis of the platypus reveals unique signatures of evolution. Nature 453:175–183

Witten G (1983) Some karyotypes of Australian agamids (Reptilia: Lacertilia). Aust J Zool 31:533–540